Article

Effect of Phosphate-Deficiency Stress on the Biological Characteristics and Transcriptomics of *Panax ginseng*

Hai Sun [1], Hao Liang [1], Cai Shao [1], Jiaqi Qian [1], Jiapeng Zhu [1], Guojia Zhang [1], Bochen Lv [1] and Yayu Zhang [1,2,*]

[1] Institute of Special Animal and Plant Science of Chinese Academy of Agricultural Science, Changchun 130112, China; sunhai@caas.cn (H.S.); lianghao20221118@163.com (H.L.); shaocai2003@163.com (C.S.); qjq15246780495@163.com (J.Q.); 18766596101@163.com (J.Z.); 15590665075@163.com (G.Z.); bochen8448@163.com (B.L.)

[2] College of Pharmacy and Biological Engineering, Chengdu University, Chengdu 610106, China

*   Correspondence: zyy1966999@sina.com; Tel./Fax: +86-043181919861

Abstract: The low availability of phosphorus has become a common problem worldwide. Phosphorus is essential for phenotypic morphology and ginsenoside synthesis. However, the effects of Pi stress on ginseng phenotype and ginsenoside synthesis remain unclear. Phenotypic analyses and transcriptomics revealed the phenotypic construction and regulation of differential genes involved in the physiological metabolism of ginseng under low-Pi stress. Root length and stem length were found to be significantly inhibited by phosphate-deficiency stress in the half-phosphate (HP) and no-phosphate (NP) treatment groups; however, the number of fibrous roots, which are regulated by phytohormones, was found to increase. In ginseng leaves, the indexes of physiological stress, superoxide anion (221.19 nmol/g) and malonaldehyde (MDA) (0.05 µmol/min/g), reached the maximum level. Moreover, chlorophyll fluorescence images and chlorophyll content further confirmed the inhibition of ginseng photosynthesis under low-Pi stress. A total of 579 and 210 differentially expressed genes (DEGs) were shared between NP and total phosphate (TP) and HP and TP, respectively, and only 64 common DEGs were found based on the two comparisons. These DEGs were mainly related to the synthesis of phosphate transporters (PHTs), phytohormones, and ginsenosides. According to KEGG analyses, four DEGs (*Pg_s 0368.2*, *Pg_s3418.1*, *Pg_s5392.5* and *Pg_s3342.1*) affected acetyl-CoA production by regulating glycometabolism and tricarboxylic acid cycle (TCA). In addition, related genes, including those encoding 13 PHTs, 15 phytohormones, and 20 ginsenoside synthetases, were screened in ginseng roots under Pi-deficiency stress. These results indicate that changes in the ginseng phenotype and transcriptional regulation of DEGs are involved in the Pi-deficiency stress environment of ginseng, thereby providing new information regarding the development of ginseng for low-Pi tolerance.

Keywords: phosphate-deficiency stress; DEGs; biological characteristics; transcriptome; ginsenosides

1. Introduction

Panax ginseng, a traditional Chinese medicinal plant, is the king of herbs in China. In fact, *P. ginseng* is widely used in oral and clinical drug therapies because of its unique pharmacodynamic components, such as ginsenosides and polysaccharides [1,2]. Interestingly, the pharmacodynamic value of ginseng is closely related to the quality of the raw material [3,4]. Quality evaluation of ginseng consists of pharmacodynamic (ginsenoside content) and sensory (root morphogenesis) evaluations [5,6]. The main production areas of ginseng are distributed throughout the Changbai Mountain and its residual veins. Notably, Jilin Province has the largest planting area. Li et al. [7] found that the available phosphorus was at the grade 3 or grade 4 level in the soil in Jilin Province. Their results were based on the nutrient classification standard of the second soil survey in China, which revealed an insufficient supply of soil-available phosphorus in the ginseng planting area.

Phosphorus, one of the three main macronutrients for plant growth, is a major component of key enzymes and secondary metabolite accumulation [8,9]. A deficiency in available phosphorus has become a common phenomenon in terrestrial ecosystems worldwide [10]. Although the total phosphorus content in the soil is high, insoluble chelates are formed by chelation with aluminum and iron in acidic soil and calcium in alkaline soil, which affects the supply of available phosphorus in the soil [11,12]. To adapt to this lower available phosphate supply in soil conditions, plants have developed phosphorus response strategies, such as changing root morphogenesis, secreting root exudates, and promoting phosphorus circulation in plants, via long-term evolution [13–15]; however, the mechanism is not clearly defined in ginseng.

Phenotypes refer to plant traits that are jointly determined or affected by the internal genetic material of crops and environmental factors, including plant growth, development, tolerance, stress resistance, physiological changes, structural formation, and yield [16]. The phenotype of plants is determined by their genetic material and external environmental conditions [17]. Owing to the complexity, variability, and dynamic changes in phenotype formation, the study of phenotypes is relatively slow. Phenotypic traits are the most intuitive expression of plant adaptation to stressful environments, and comprehensive and accurate phenotypic information is essential to perform in-depth evaluations on the function of related genes and reveal their regulatory networks [18,19].

MDA, a critical index of plasma membrane damage and plant senescence, can be regarded as a physiological index of stress because its reaction with biomacromolecules leads to an increase in reactive oxygen species (ROS) in the plasma membrane, which changes the fluidity and permeability of cell membranes and damages the normal physiological function of the cell. The superoxide anion production rate (O_2^- rate), another important index of plasma membrane damage and plant senescence, has immune and signal transduction functions. For example, the superoxide anion damages the structure and function of the cell membrane, leading to abnormal metabolism of cells and tissues when accumulation exceeds the defense capacity of the organism. MDA and superoxide anions have been used as indicators of cell and tissue damage under phosphorus starvation in *Arachis hypogaea* L. [20] and *Neolamarckia cadamba* [21]. Phosphorus deficiency also weakens the photosynthetic capacity of leaves owing to the plasma membrane damage caused by the overproduction of ROS [22].

Recently, several studies have focused on the interactions between biological characteristics and differential genes under phosphorus deficiency in rice [23], maize [24], soybean [25], and cotton [26] by leveraging the transcriptome. However, the mechanisms underlying the relationship between the biological characteristics and transcriptomics of phosphate-deficiency stress in *Panax ginseng* remains unknown.

Therefore, studying the physiological response and activating or inhibiting the effects of related genes under phosphate deficiency in ginseng is of great significance. We hypothesized that (1) changes in phenotypic and physiological indices might be caused by phosphorus deficiency. Accordingly, MDA and superoxide anion production rates were induced to resist adversity and stress. (2) Some related genes were overexpressed or downregulated under low-phosphorus stress; and (3) the synthesis and accumulation of secondary metabolites in ginseng, such as phosphate transporters (PHTs), phytohormones, TCA, and ginsenoside, may be regulated by Pi-deficiency stress.

2. Materials and Methods

2.1. Experimental Design

This experiment was performed in an innovative training room at the Institute of Special Animal and Plant Science of CAAS. After germination of physiologically ripe ginseng seeds for 1 day at room temperature, they were transferred onto a filter paper soaked in distilled water, placed in a tray, sealed, and transferred to breeding plates after 3 days in a hydroponic device equipped with deionized water. When the stem grew to approximately 3 cm after 3 days, 30 seedlings of approximately the same size were selected

and transferred to the pre-prepared plastic plate (59 cm $\times$ 11 cm) with holes (1.7 cm in diameter) for seeding training in special nutrient solution with HBO_3 (8 μmol·L^{-1}, $CaCl_2$ 50 μmol·L^{-1}). The seedlings were allowed to adapt for 3 days in a hydroponic device. Thereafter, the endosperm was manually removed to eliminate nutrients carried by the mother. The temperature range of the culture chamber was 23–28 °C, the humidity was controlled between 60 and 70%, the light intensity was 105 mol m^{-2} s^{-1}, and the photoperiod was 12 h. A total of 300 seedlings were prepared.

The prepared ginseng seedlings were cultured in Hoagland nutrient solution with different concentrations of phosphate (NP, 0 mg·L^{-1}; HP, 68 mg·L^{-1}; TP, 136 mg·L^{-1}). The PO_4^{3-} supply was adjusted using KCl and KH_2PO_4; the pH was adjusted to 6.0 $\pm$ 0.1; and the nutrient solution was changed every 3 days. Samples were collected after 15 days of stress treatment, and their biomass (fresh weight and dry weight) was recorded.

2.2. Determination of Leaflet Area, Physiological Indices, Root Morphogenesis, and Phosphorus

Three random ginseng seedlings were selected to measure the leaflet area. The leaflet area was calculated using the analysis parameter values of 0.063 and 0.765, and a MAXI-PAM portable modulated chlorophyll fluorescence analyzer (WALZ, Wurzburg City, Germany), which was fully light-adapted before measurement. Dark treatment was then performed for 40 min and repeated three times.

The MDA content and superoxide anion content (O_2^- rate) were determined using a malondialdehyde content assay kit and superoxide anion content assay kit (superoxide anion content), respectively, in accordance with the manufacturer's instructions. The detailed steps are in accordance with those of a previous study [27].

The ginseng root morphological index was analyzed using a root system analysis equipment (WinRHIZO; Regent Instruments Inc., Québec City, QC, Canada). Briefly, the ginseng root was washed with water, drained, and placed in a clean high-penetration scanning dish. The position of the root system was adjusted to maximize extension of the root system in the dish. A root scanner (EPSON1680 for grey scanning at 400 dpi) was used. The WinRHZIO root analysis system was employed to calculate the total root length, projection area, surface area, diameter, and volume [28].

The phosphate content in different parts of ginseng was determined via acid digestion and the molybdenum antimony resistance colorimetric method [29].

2.3. RNA Extraction, Illumina Sequencing, and Transcriptome Data Analysis

Thirty seedlings from each of the NP, HP, and TP groups were divided into three groups (three biological replicates). The roots were used for RNA-Seq, which was performed by Shanghai OE Biotech Co., Ltd (Shanghai, China). RNA was extracted, quantified, and sequenced as described by Shen et al. [30]. The quality of the sequenced RNA was verified using libraries on an Illumina platform.

2.4. Identification of DEGs

To quantify gene expression, a feature-count-based approach was used. Transcript counts were performed using DESeq2 for differential gene expression analyses. Corrected p-value < 0.05 and $|\log_2 \text{foldchange}| > 2$ were used as the thresholds.

2.5. Determination of Ginsenoside Content

A total of 1.00 g powder of ginseng root and leaf were weighed, respectively, and ultrasonically extracted for 30 min with 20 mL 95% methanol; sonication was repeated three times. The contents of 10 ginsenosides, including PPD ginsenosides Rb_1, Rb_2, Rb_3, Rc, and Rd; PPT ginsenosides Rg_1, Re, Rf, and Rg_2; and OA ginsenoside Ro, were determined using HPLC (high-performance liquid chromatography (HPLC; H-Class, Waters, Milford, MA, USA) analysis based on the Chinese Pharmacopeia 2020 edition [31,32].

2.6. Statistical Analysis and Drawing

All data in the tables and figures are presented as mean ± standard deviation. Bar graph was generated using GraphPad Prism 6 to explore the differences in phosphorus deficiency among the NP, HP, and TP treatment groups. Significant differences between different treatments were analyzed according to Fisher least significant difference (Fisher-LSD) post hoc test at $p < 0.05$ on SAS 9.0. Bioinformatic analysis was performed using the OECloud tool (https://cloud.oebiotech.com/task/, accessed on 20 July 2022). A volcano map (or other graphics) was generated using R (https://www.r-project.org/, accessed on 20 July 2022) on the OEC cloud platform (https://cloud.oebiotech.com/task/, accessed on 20 July 2022). All image combinations were derived using Adobe Illustrator 2021 software.

3. Results

3.1. Effect of Phosphate Deficiency on the Biological Characteristics of Ginseng

Root and stem lengths were significantly reduced under phosphate deficiency (Table 1 and Figure 1B). Root length in the NP and HP treatment groups was smaller than that in the TP group ($p < 0.05$); however, no significant difference in root length was found between the NP and HP treatment groups. Shoot length was the highest with TP treatment (7.90 cm), followed by HP and NP treatments. Notably, significant differences were found among the different treatment groups. Although root elongation and expansion were significantly inhibited under phosphate deficiency, no significant discrepancy was found in the average leaflet area.

Table 1. Effect of phosphate deficiency on root length, shoot length, and average leaflet area.

Treatments	Root Length (cm)	Shoot Length (cm)	Average Leaflet Area (cm^2)
NP	4.36 ± 0.08 b	5.42 ± 0.31 c	4.53 ± 0.16 a
HP	4.35 ± 0.06 b	6.41 ± 0.22 b	3.52 ± 0.21 a
TP	5.26 ± 0.28 a	7.90 ± 0.48 a	4.89 ± 0.22 a

Note: Data are presented as mean ± standard error ($n = 3$). Lowercase symbols among the NP, HP, and TP treatment groups indicate significance at $p < 0.05$.
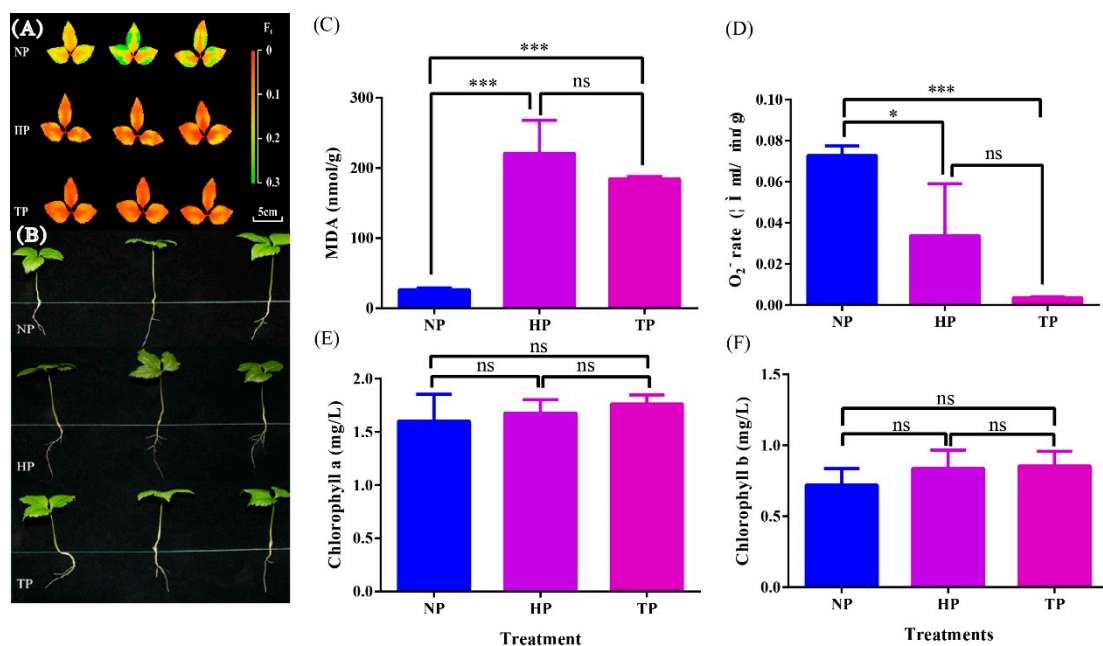

Figure 1. Effect of phosphate deficiency on chlorophyll fluorescence (**A**), biological characteristics (**B**), malondialdehyde content (**C**), O_2^- rate (**D**), chlorophyll a (**E**), and chlorophyll b (**F**) of ginseng. Significant levels are indicated by * $p < 0.05$ and *** $p < 0.001$; ns indicates $p > 0.05$.

Growth stress in ginseng leaves was detected using a chlorophyll fluorescence analyzer (Figure 1A). The chlorophyll fluorescence image indicates the degree of stress induced by P deficiency on photosynthesis in ginseng leaves. The chlorophyll fluorescence in the TP treatment group was bright and reddish while that in the HP treatment group was slightly dark and green at the edge of leaves. For the NP treatment group, a large area of green fluorescence was observed. This phenomenon indicates that the photosynthetic efficiency and electron transfer ability of ginseng leaves were severely inhibited by NP treatment. The contents of chlorophyll a and b were the highest in the TP treatment group, followed by the HP and NP treatment groups; however, no significant difference was found among the treatment groups.

In general, MDA and the superoxide anion production rate (O_2^- rate) can be regarded as physiological indices of the degree of stress. The content of MDA was 221.19 nmol/g in the HP treatment group; this value was significantly higher than that in the NP treatment group ($p < 0.001$) (Figure 1C). The O_2^- rate was the highest in the NP treatment group, followed by the HP and TP treatment groups, and significantly different at a P level of 0.05 (Figure 1D). However, the chlorophyll a and b contents were not significantly different among the treatment groups (Figure 1E,F).

Figure 2 shows that ginseng root morphogenesis was affected by phosphate deficiency. Root elongation and expansion were distinctly inhibited and the number of fibrous roots markedly decreased in the NP treatment group. Significant differences in root length, root project area, root surface area, and average diameter were found between the TP/NP and NP treatment groups ($p < 0.05$) (Table 2).
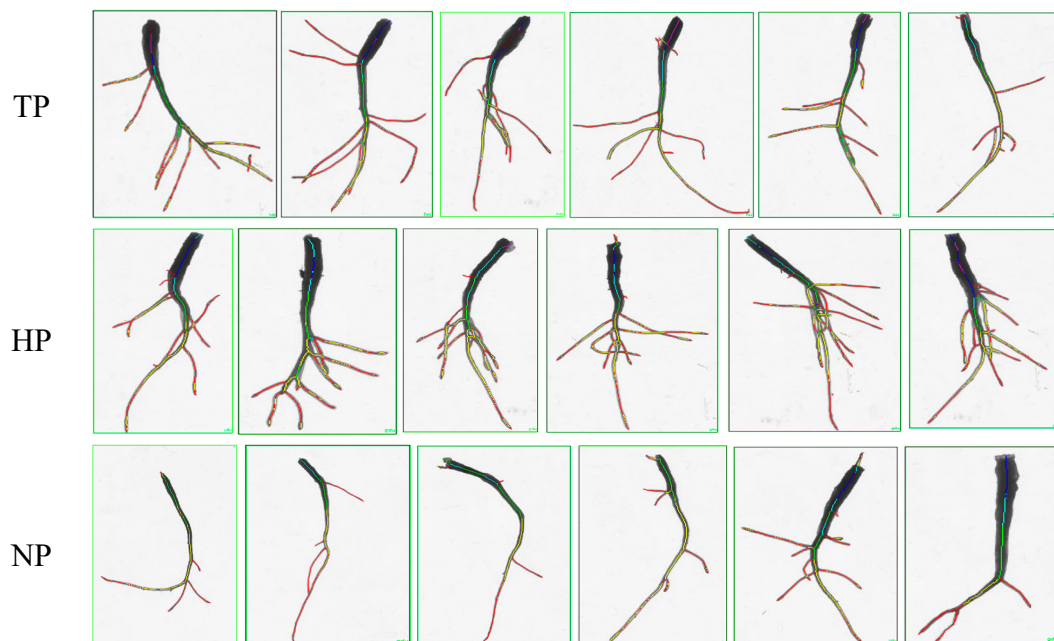

Figure 2. Effect of phosphate deficiency on root morphogenesis of ginseng.

Table 2. Effects of different phosphate concentrations on ginseng root morphogenesis.

Treatments	Total Root Length (cm)	Root Project Area (cm^2)	Root Surface Area (cm^2)	Average Diameter (mm)	Later Root Amount
NP	6.28 ± 0.68 b	1.37 ± 0.19 b	2.87 ± 0.58 a	0.44 ± 0.06 b	5.83 ± 1.61 a
HP	10.29 ± 0.98 a	2.57 ± 0.21 a	2.97 ± 0.18 a	0.78 ± 0.07 a	8.17 ± 0.98 a
TP	11.88 ± 1.43 a	2.76 ± 0.42 a	3.22 ± 0.45 a	0.89 ± 0.13 a	4.33 ± 1.75 a

Note: Data are presented as mean ± standard error (n = 3). Lowercase symbols among the NP, HP, and TP treatment groups indicate significance at $p < 0.05$.

3.2. Effect of Phosphate Deficiency on the Transcriptome of Ginseng

We obtained 47.13–51.07 million raw reads, more than 6.47 GB of clean bases, and 47 million clean reads per library from 9 ginseng samples via transcriptome sequencing (Table S1). The GC content ranged from 44.91 to 45.18, the Q30 of the clean reads was greater than 92.68%, and the total mapped ratios were greater than 96.79%. The results indicate that the transcriptomic data were satisfactory for further analyses.

Differential expression analysis was conducted to identify the differentially expressed genes related to phosphorus deficiency in ginseng (Figure 3). With respect to the degree of phosphorus stress, 579 and 210 DEGs were found to be shared between NP and TP, and HP and TP, respectively. Only 64 common DEGs were found from the 2 comparisons. The volcanic map results revealed that 248 and 78 DEGs were upregulated while 395 and 196 DEGs were downregulated in the NP vs. TP and HP vs. TP groups, respectively.

We explored the functional discrepancy between DEGs under low-phosphate stress conditions (Tables S2 and S3). GO and Kyoto Encyclopedia of Genes and Genomes (KEGG) enrichment analyses were performed to identify the potential functions of the DEGs. The top 30 components in the 3 functional categories (biological process (BP), cellular component (CC), and molecular function (MF)) between the NP and TP, and HP and TP groups based on the level 2 GO term assignment are shown in Figure 4. The top 10 processes, including response to salicylic acid, negative regulation of phosphorylation, positive regulation of phosphatase activity, metaphase/anaphase transition of mitotic cell cycle, starch biosynthetic process, abscission, fructose metabolic process, lipid catabolic process, carbohydrate biosynthetic process, and response to lithium ion, were the biological processes identified in the HP vs. TP group comparison. In contrast, salicylic acid catabolic process, phosphate ion transport, terpenoid biosynthetic process, cellular response to phosphate starvation, response to lithium ion, positive regulation of cellular response to phosphate starvation, response to oxidative stress, response to abscisic acid, glycerol metabolic process, and cellular phosphate ion homeostasis were the identified biological processes in the NP vs. TP group comparison. Among them, four processes were related to P metabolism, two processes were related to plant phytohormone response, and two processes were related to carbohydrate metabolism in the HP vs. TP group. Five processes were related to P metabolism, two processes were related to plant hormone response, one process was related to the terpenoid biosynthetic process, and one process was related to PHTs in the NP vs. TP group. The cellular components and molecular functions differed between the HP vs. TP and NP vs. TP groups.

The DEGs in response to P stress are shown in volcano plots (Figure 3C,D). The DEGs were classified using KEGG pathways. The physiological processes of "plant hormone signal transduction" and "MAPK signaling pathway" were annotated in the response to P stress between the HP vs. TP and NP vs. TP groups. These processes may be associated with genes, such as *Pg_S2566.5*, *Pg_S4931.9*, *Pg_S5077.6*, *Pg_S5602.1*, and *Pg_S6397.3* in HP vs. TP and *Pg_S1844.26* in NP vs. TP (Tables S4 and S5). The most represented pathways were pentose and glucuronate interconversion, amino sugar and nucleotide sugar metabolism, and starch and sucrose metabolism in the HP vs. TP groups. In contrast, phenylpropanoid biosynthesis and glycolysis/gluconeogenesis were most represented in the NP vs. TP groups. Some common metabolic pathways, including plant hormone signal transduction; cute, suberin, and wax biosynthesis; pentose and glucuronate interconversions; carotenoid biosynthesis; glycolysis/gluconeogenesis; the tricarboxylic acid cycle (TCA cycle); and carbon fixation in photosynthetic organisms, were also found.
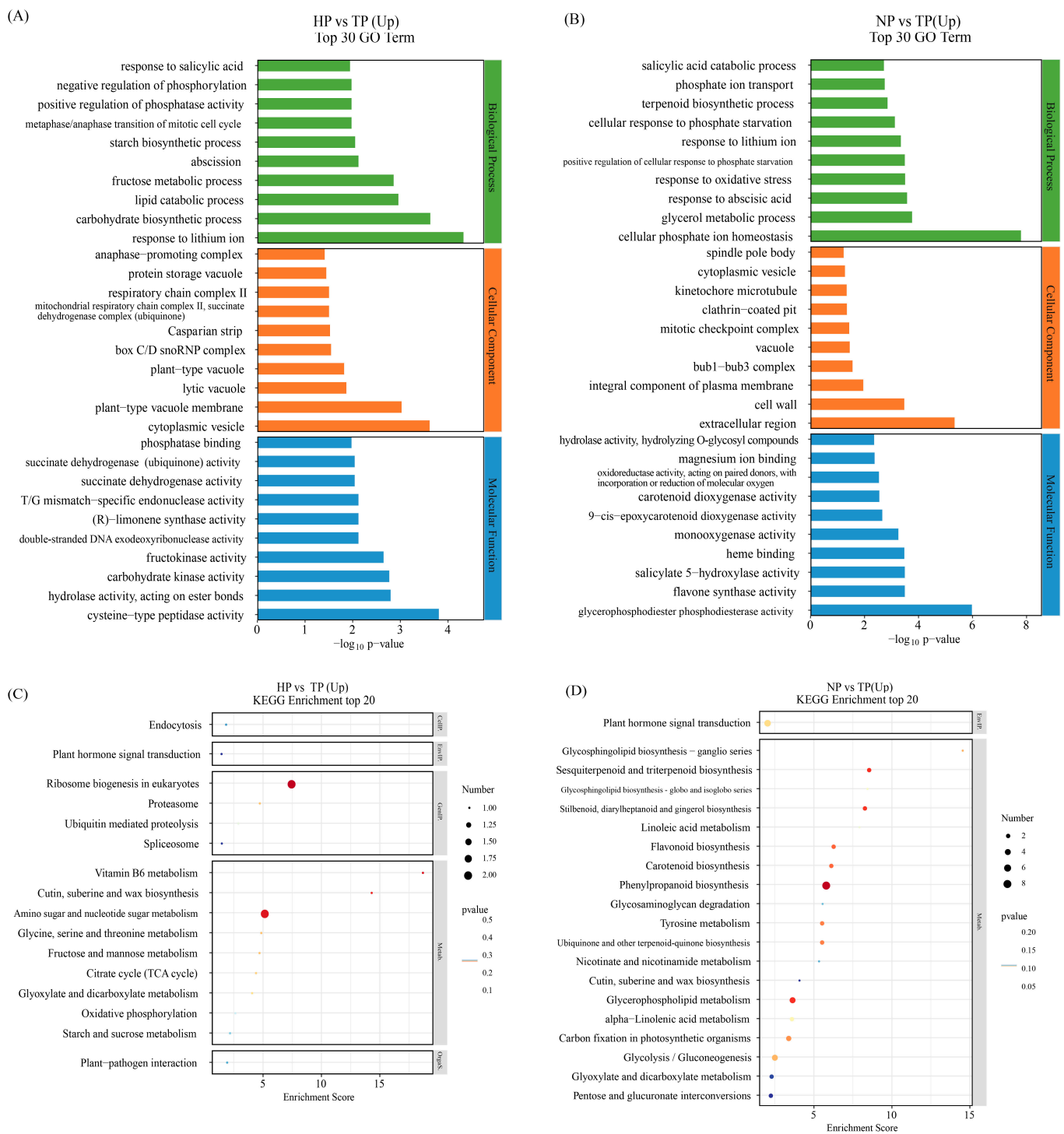
Figure 3. Effect of phosphate deficiency on DEGs. (**A**) Venn diagram, (**B**) different gene statistic, (**C**) volcano plot between the NP and TP treatment groups, (**D**) volcano plot between the HP and TP treatment groups.

Figure 4. GO and KEGG pathway enrichment analyses based on DEGs. GO classifications revealed upregulated gene categories in the HP vs. TP (**A**) and NP vs. TP (**B**) groups. KEGG enrichment analysis of upregulated differentially expressed genes in the HP vs. TP (**C**) and NP vs. TP (**D**) groups.

3.3. Relative Genes in the Synthesis of PHTs, Ginsenoside, and Phytohormone

Many DEGs were involved in PHT synthesis, ginsenoside synthesis, and phytohormone signaling. A total of 34 genes (21 upregulated genes and 13 downregulated genes) were identified in the NP and TP groups, whereas 36 genes (14 upregulated genes and 22 downregulated genes) were identified in the HP vs. TP groups. A total of 13 commonly upregulated genes, *Pg_S0061.26*, *Pg_S5840.2*, *Pg_S0543.4*, *Pg_S2015.28*, *Pg_S0073.19*,

Pg_S0129.2, *Pg_S2306.7*, *Pg_S3149.14*, *Pg_S2984.3*, *Pg_S3048.21*, *Pg_S0519.15*, *Pg_S0302.39*, and *Pg_S0917.29*, were identified as potential target genes that might be involved in phosphorus transport (Figure 5).
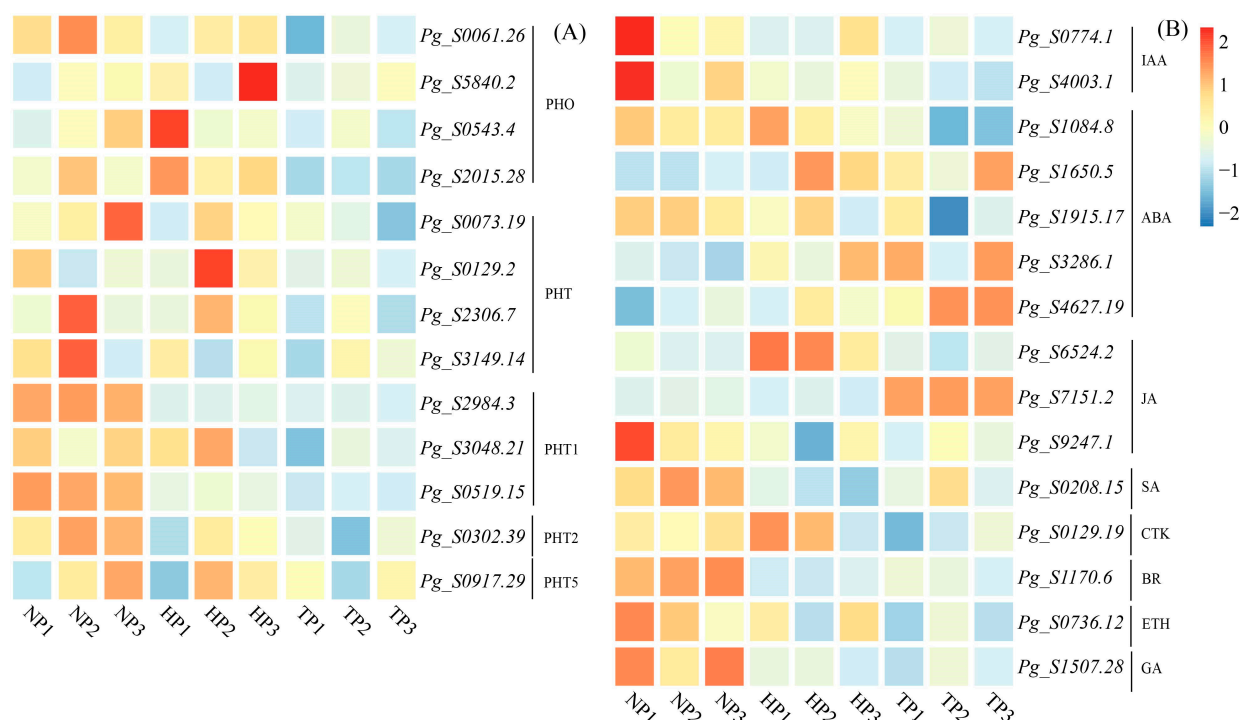

Figure 5. Heatmap of DEGs associated with phosphate transporter (**A**) and phytohormone signal transduction (**B**). The red and blue boxes represent genes upregulated and downregulated under different P stress conditions. Abbreviations: PHO, Phosphate; PHT, Phosphate transporter; PHT1, Phosphate transporter 1; PHT2, Phosphate transporter 2; PHT5, Phosphate transporter 5; IAA, Indole-3-acetic acid; ABA, Salicylic acid; JA, Jasmonic acid; SA, Salicylic acid; CTK, Cytokinin; BR, Brassinolide; ETH, Ethylene; GA, Gibberellin.

A total of 20 potential genes related to key rate-limiting enzymes in P stress were identified, including AACT (*Pg_S6240.3*), HMGS (*Pg_S4594.4*), HMGR (*Pg_S2025.5*), MVK (*Pg_S3098.25*, *Pg_S3551.1*, *Pg_S4382.5*, *Pg_S3098.25*, *Pg_S3551.1*, *Pg_S4382.5*), MVD (*Pg_S1430.1*), FPS (*Pg_S5797.2*), SE (*Pg_S4043.9*), β-AS (*Pg_S2225.7*, *Pg_S2801.2*, *Pg_S4815.4*), and UGTs (*Pg_S1661.1*, *Pg_S1712.22*, *Pg_S1924.2*, *Pg_S3672.12*, *Pg_S4880.11*). These genes were upregulated in the NP and HP treatment groups compared to those in the TP treatment group and may promote ginsenoside synthesis.

A total of 15 DEGs involved in phytohormone signal transduction were identified in all treatment groups, including IAA (*Pg_S0774.1*, *Pg_S4003.1*), ABA (*Pg_S1084.8*, *Pg_S1650.5*, *Pg_S1915.17*, *Pg_S3286.1*, *Pg_S4627.19*), JA (*Pg_S6524.2*, *Pg_S7151.2*, *Pg_S9247.1*), SA (*Pg_S0208.15*), CTK (*Pg_S0129.19*), BR (*Pg_S1170.6*), ETH (*Pg_S0736.12*), and GA (*Pg_S1507.28*).

3.4. Expression Pattern of Relative Gene in the Biosynthesis Pathway of TCA and Ginsenoside Synthesis

Some essential genes related to key rate-limiting enzymes of triterpenoid synthesis have been reported in ginseng roots [33]. We found that 4 DEGs and 17 upregulated genes were related to the TCA cycle and ginsenoside synthesis under P stress. A heatmap was generated based on the DEGs between the NP vs. TP and HP vs. TP groups (Figure 6).
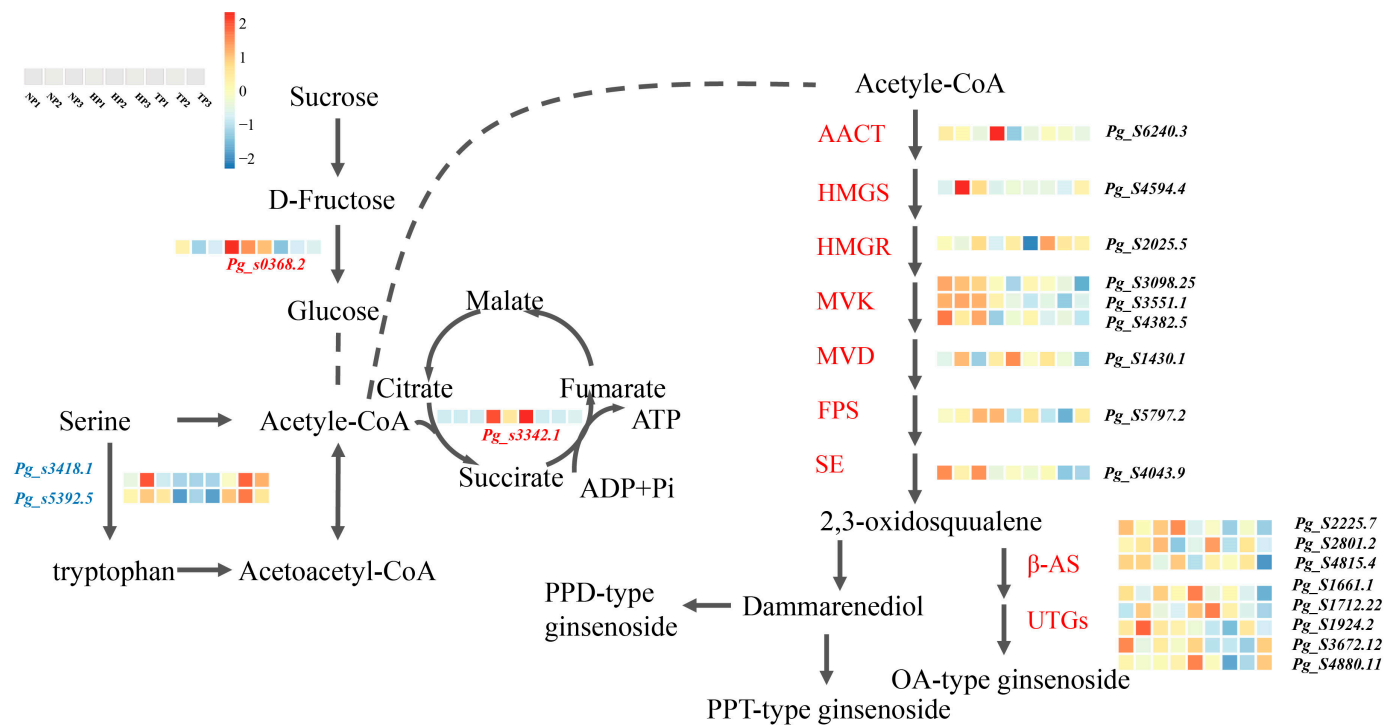
Figure 6. Expression profiles of DEGs associated with TCA and ginsenoside synthesis. Abbreviations, AACT, acetyl-CoA C-acetyltransferase; HMGS, hydroxy methylglutaryl-CoA synthase; HMGR, hydroxy methylglutaryl-CoA reductase; MVK, mevalonate kinase; MVD, mevalonate diphosphate decarboxylase; FPS, farnesyl diphosphate synthase; SE, squalene epoxidase; β-AS, β-amyrin synthase; UGTs, UDP-glucuronosyltransferase.

3.5. Effect of Phosphate Deficiency on Ginsenoside Accumulation

To assess ginsenoside accumulation and distribution aboveground and belowground under different phosphorus deficiency conditions, the total ginsenosides and 10 ginsenoside monomers were analyzed in ginseng roots and leaves among the NP, HP, and TP treatment groups (Figure 7). The NP treatment group had the highest contents of Rg_1, Re, Rf, Rc, Rb_2, Rd, and total ginsenosides in ginseng roots, followed by the HP and TP treatment groups. The Rg_1, Ro, Rb_2, Rb_3, and total ginsenosides were significantly different at 0.01 or 0.05 among the NP, HP, and TP treatment groups. However, the contents of Rg_1, Rb_3, Rd, and total ginsenosides in ginseng leaves were highest in the NP treatment group, followed by the TP and HP treatment group. Moreover, the contents were remarkably different among the different treatment groups ($p < 0.05$). Interestingly, the TP treatment group had the highest contents of Re, Rf, Rg_2, Ro, and Rc, followed by the NP and HP treatment groups, with significant difference found at $p < 0.05$. In addition, the ratios of PPT and PPD were similar in the roots and leaves of ginseng, and in the HP, TP, and NP treatment groups, in descending order.
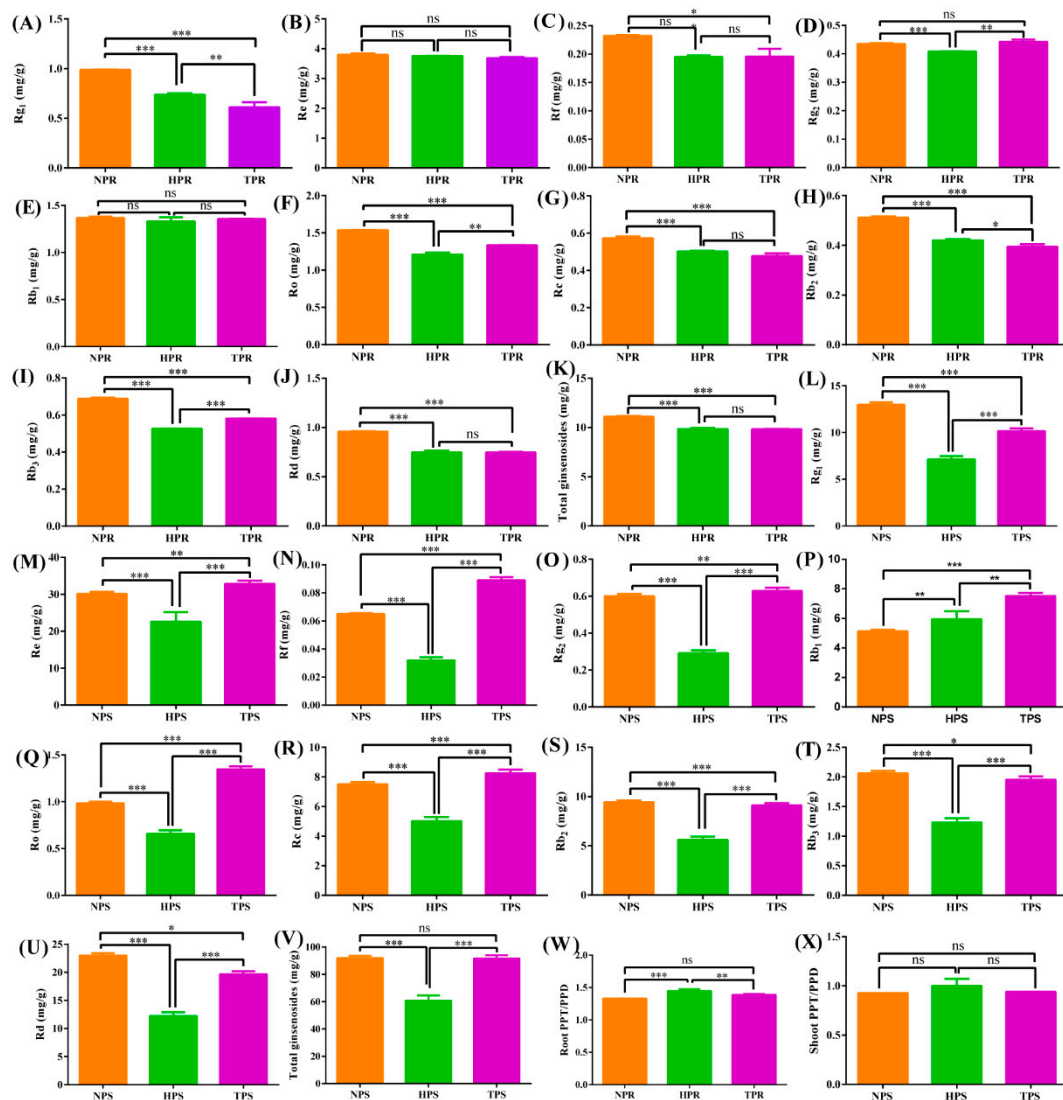
Figure 7. Effect of phosphate deficiency on ginsenoside accumulation and PPT/PPD in root and shoot. The symbols *, **, and *** indicate significant difference in ginsenoside or PPT/PPD among the different treatment groups at 0.05, 0.01, and 0.001, respectively. (**A**) Rg_1 in root, (**B**) Re in root, (**C**) Rf in root, (**D**) Rg_2 in root, (**E**) Rb_1 in root, (**F**) Ro in root, (**G**) Rc in root, (**H**) Rg_2 in root, (**I**) Rb_3 in root, (**J**) Rd in root, (**K**) Total ginsenosides in root, (**L**) Rg_1 in shoot and leaf, (**M**) Re in shoot and leaf, (**N**) Rf in shoot and leaf, (**O**) Rg_2 in shoot and leaf, (**P**) Rb_1 in shoot and leaf, (**Q**) Ro in shoot and leaf, (**R**) Rc in shoot and leaf, (**S**) Rg_2 in shoot and leaf, (**T**) Rb_3 in shoot and leaf, (**U**) Rd in shoot and leaf, (**V**) Total ginsenosides in shoot and leaf, (**W**) PPT/PPD in root, and (**X**) PPT/PPD in shoot and leaf.

4. Discussion

4.1. Phosphate Stress Changes Ginseng Root Morphogenesis and Triggers the Expression of Different Genes

The deficiency of available phosphorus in soil has become a worldwide concern [34,35]. To adapt to the stressful environment of phosphorus deficiency, a series of strategies, such as changing root morphogenesis and biomass accumulation, trigger gene expression related to phosphorus uptake, absorption, and transport in plants [36–38]. Our study revealed that the growth of ginseng under P stress was restricted (above- and belowground). The lengths of the roots and shoots in the HP and NP treatment groups were markedly lower than those in the NP treatment group. This result is consistent with that found in previous studies on other crops, such as alfalfa [15], *Leymus chinensis* [39], *nicotiana tabacum* [40], etc. This finding is mainly due to the role of P as an essential structural component of

membrane phospholipids, nucleic acids, and adenosine phosphoric acid, and its effects on normal growth, development, and biomass accumulation [15,41].

The phenotype of chlorophyll fluorescence F_o (fluorescence origin) can visually indicate, to a certain extent, the degree of biotic or abiotic stress and the extent of photosynthetic damage to plants [42,43]. The F_o image of ginseng leaves from the HP and NP treatment groups revealed different areas with green fluorescence, indicating that the photosynthesis of ginseng leaves was affected, to some extent, by the different phosphate stress conditions. F_o is the fluorescence yield (basal fluorescence or 0-level fluorescence) when the photosystem II (PSII) reaction center is fully open and is related to the leaf chlorophyll content [44]. Based on our results, the contents of chlorophyll a and b were the highest in the TP treatment group, followed by the HP and NP treatment groups, aligning with the results of the phenotypic analysis.

Plant physiological indicators, especially MDA and superoxide anion accumulation, are considered the most sensitive indicators of plant stress and have been used in many environmental stress studies as key indicators [45,46]. MDA, one of the most important products of membrane lipid peroxidation, can be used to indirectly determine the degree of damage to the membrane system and tolerance to stress in plants [47,48]. The MDA content was found to significantly increase under moderate phosphorus deficiency (HP treatment) and significantly decrease under phosphorus starvation (NP treatment) conditions (Figure 1C). Such a finding indicates that the accumulation of ROS activates the self-defense ability of ginseng within a certain stress range, resulting in an increase in MDA content. However, excessive ROS accumulation causes membrane damage and a lack of self-mediation in ginseng. The over-accumulation of superoxide anions further explained the plasma membrane peroxidation in ginseng (Figure 1D). Additionally, MDA and H_2O_2 at nanomolar concentrations also serve as vital signaling molecules that enable plant cells to rapidly respond to adverse environmental conditions [49].

Plant morphogenesis, especially root morphogenesis, is closely related to P supply [50]. Under low-P stress (HP or NP), the growth of ginseng roots and shoots was found to be stunted; however, the growth of lateral roots was promoted (Tables 1 and 2, Figure 2). This result is consistent with that of previous studies on wheat [36] and rice [51]. The possible mechanism may involve the triggering of the upregulation or downregulation of related genes under phosphorus deficiency signals to maintain phosphorus homeostasis in plant growth, which further induces the differential expression of hormones and related enzymes, ultimately causing changes in plant morphogenesis [52].

4.2. Multiple DEGs Are Involved in PHTs and Phytohormone Signal Transduction

Several physiological and metabolic responses are activated to adapt to adverse environments when plants are exposed to abiotic stressors [53]. P is a key component of many metabolites and macromolecules, including adenosine triphosphate (ATP), proteins, membrane phospholipids, and nucleic acids, and is involved in many biochemical pathways, such as energy transmission, gene expression, and signal transduction [54]. In this study, some genes related to ginseng morphogenesis were found to be triggered by P deficiency, especially those involved in PHTs, phytohormone signal transduction, and ginsenoside synthesis.

Thirteen common genes related to PHTs were found in ginseng under P stress treatment, of which the relevant coding gene families mainly included PHO, PHT, PHT1, PHT2, and PHT5 (Figure 5A). Previous studies confirmed that two main types of proteins related to PHTs exist: PHTs and PHOs. The PHTs family mainly includes PHT1, PHT2, PHT3, and PHT4, located on the plasma membrane, mitochondria, chloroplasts, and Golgi apparatus, respectively. In contrast, PHO mainly transports Pi from the roots to stems, which is not homologous to the PHT family [55,56]. The encoding genes, PHTs and PHOs, were found in ginseng under low-phosphate stress, and may be involved in phosphate transport under low-phosphorus stress. However, the underlying mechanism must be further studied.

Phytohormones participate in root morphogenesis under low-phosphorus stress [57]. Compared to CK (TP), the related genes encoding IAA, CTK, and ETH in ginseng roots were upregulated under low-P stress (HP), and more genes were upregulated under phosphorus starvation (NP), mainly including the genes encoding IAA, SA, CTK, BR, ETH, and GA. IAA has been confirmed to be involved in the root system architecture (RSA) under P stress, particularly in the inhibition of primary root growth and proliferation of lateral roots and root hairs [58]. The gene expression of CTK plays an essential role in plant growth and development and negatively regulates Pi deficiency tolerance by modulating PHTs [59]. Figure 2 shows that moderate Pi deficiency (HP treatment) inhibited primary root growth and promoted lateral root growth. These results are consistent with those of previous studies on rice [60], sorghum [61], and Arabidopsis [62] under Pi-deficient conditions. One possible mechanism may involve the activation of H^+-ATPase activity and H^+ secretion by ethylene signals in the morphological regulation of ginseng roots, thereby enhancing Pi absorption [63]. However, the synergistic mechanisms of different phytohormones in ginseng are complex and may involve other regulatory mechanisms to balance internal phosphorus homeostasis.

4.3. Multiple DEGs Are Involved in TCA and Ginsenoside Synthesis

Phosphorus is a plant skeleton element that participates in the physiological processes of energy and carbohydrate metabolism and regulates metabolic processes [64]. TCA is the final pathway of sugars, lipids, and amino acids that maintains the stability of carbon metabolism in plants under abiotic stress and is essential for plant growth and stress tolerance [65,66]. We found that the downregulated expression of *Pg_s3418.8* and *Pg_s5392.5* caused serine accumulation in the cyclic, serine, and threonine metabolism, and accelerated the process of acetyl-CoA production. In addition, *Pg_s3342.1*, a key succinate dehydrogenase gene, was upregulated under phosphate stress in ginseng, promoting the formation of fumarate and ATP in the TCA pathway. This result may be due to a disruption in the dynamic balance between ROS accumulation and clearance under low-phosphorus stress. To remove excess ROS, some genes related to carbon metabolism and ATP supply via the TCA pathway are overexpressed [67].

Ginsenoside accumulation is co-regulated by key enzymes and environmental factors. Ginsenosides can be divided into three types: PPT-, PPT-type-, and OA-type ginsenosides [68]. Under low-Pi stress, the ratio of PPT/PPD increased in the roots and stems of ginseng and was significantly higher in the HP treatment group than in the TP or NP treatment groups (Figure 7). This result indicates that low-Pi stress promoted the synthesis of PPT and inhibited the synthesis of PPD, possibly because low-Pi stress induced the upregulated expression of genes related to PPT synthesis. Ginsenoside accumulation is regulated by numerous ginsenoside synthesis genes in the saponin synthesis pathway, including 3-hydroxy-3-methylglutaryl CoA reductase (HMGR), squalene synthase (SS), squalene epoxidase (SE), dammarenediol synthase (DS), cytochrome P450, and glycosyltransferase (GT) [69]. In this study, the contents of Rg_1 and Rb_2 were significantly higher in the low-Pi groups (NP and HP) than in the total phosphate treatment (TP) group, with 17 related upregulated genes of ginsenoside synthetase identified in ginseng roots under low-Pi supply (Figure 6). The gene, *Pg_s6240.3*, which encodes the limited AACT enzyme, was upregulated in the low-Pi treatment group, which is consistent with the results of previous studies on drought stress in ginseng; this gene could promote the accumulation of ginsenoside Rb_2 [32]. The β-AS enzyme coding genes, *Pg_s2801.2* and *Pg_s4815.4*, were also found in ginseng root under low-Pi stress, and expression of the two genes was found to contribute to ginsenoside biosynthesis, aligning with the increased contents of dammarenediol-type ginsenosides caused by the upregulation of the β-AS enzyme [70]. In addition, several unreported genes of key-limited enzymes for ginsenoside synthesis were found under low-Pi stress, including *Pg_s4594.4*, *Pg_s2025.5*, *Pg_s3098.25*, *Pg_s 3551.1*, *Pg_s 4382.5*, *Pg_s 1430.1*, *Pg_s 5797.2*, *Pg_s 4043.9*, *Pg_s 2225.7*, *Pg_s 1661.1*, *Pg_s 1712.22*, *Pg_s 3672.12*, and *Pg_s 4880.11*, which may help further clarify the pathway of ginsenoside

biosynthesis. The ginsenosides, Rg_1, Rf, Ro, Rc, Rb_2, Rb_3 Rd, total ginsenosides in ginseng root, were higher in NP than that in TP. The results are in agreement with common sage (*Salvia officinalis*), the possible metabolism is that overexpression of GA related gene could promote the synthesis of triterpenoids [71].

Based on the screened DEGs, the regulatory networks among differential genes, hormones, ginseng root morphogenesis, and ginsenoside synthesis were mapped and verified in the future study, which elucidates the mechanism of phytohormone-mediating root morphogenesis and secondary metabolites synthesis in ginseng under low-phosphorus stress.

5. Conclusions

Phenotypic and transcriptomic analyses were performed to explore the physiological response mechanisms of low-Pi tolerance in ginseng. Root length and stem length were significantly inhibited by Pi-deficiency stress; however, the number of fibrous roots increased. Meanwhile, superoxide anions and MDA were induced to rebalance ROS accumulation and elimination in ginseng under Pi-deficiency stress. Several genes were found in ginseng roots; these genes are mainly related to the synthesis of PHTs, phytohormones, and ginsenosides, and are involved in root morphogenesis, TCA, and ginsenoside synthesis. To our knowledge, this study is the first to identify some of the DEGs presented herein. Moreover, this study provides new information regarding the development of ginseng with low-Pi tolerance.

Supplementary Materials: The following supporting information can be downloaded at: https://www.mdpi.com/article/10.3390/horticulturae10050506/s1, Table S1: Summary of RNA-Seq results; Table S2: the top 30 of up regulated DEGs of gene ontology in group HP vs. TP; Table S3: the top 30 of up regulated DEGs of gene ontology in group NP vs. TP; Table S4: the top 20 of up regulated DEGs of KEGG in group HP vs. TP; Table S5: the top 20 of up regulated DEGs of KEGG in group NP vs. TP.

Author Contributions: H.S. carried out the experimental plan and revised the manuscript. H.L. extracted DNA and conducted data analysis. C.S., J.Q., J.Z., G.Z. and B.L. collected the samples and performed experiments. C.S. participated in the experimental design, and drafted the manuscript. Y.Z. revised the manuscript and provide financial support. All authors have read and agreed to the published version of the manuscript.

Data Availability Statement: Data are contained with in the article and supplementary materials.

Conflicts of Interest: The authors declare that they have no known competing financial interests or personal relationships that could have appeared to influence the work reported in this paper.

References

1. Yi, Y.S. Pharmacological potential of ginseng and ginsenosides in nonalcoholic fatty liver disease and nonalcoholic steatohepatitis. *J. Ginseng Res.* **2024**, *48*, 122–128. [CrossRef]
2. Cecarini, V.; Cuccioloni, M.; Gong, C.M.; Liu, Z.Q.; Bonfili, L.; Angeletti, M.; Angeloni, S.; Alessandroni, L.; Sagratini, G.; Liu, H.M.; et al. Role of Panax ginseng and ginsenosides in regulating cholesterol homeostasis. *Food Biosci.* **2023**, *56*, 103256. [CrossRef]
3. Ma, R.; Yang, P.D.; Jing, C.X.; Fu, B.Y.; Teng, X.Y.; Zhao, D.Q.; Sun, L.W. Comparison of the metabolomic and proteomic profiles associated with triterpene and phytosterol accumulation between wild and cultivated ginseng. *Plant Physiol. Biochem.* **2023**, *195*, 288–299. [CrossRef]
4. Kan, H.; Zhang, D.X.; Chen, W.J.; Wang, S.H.; He, Z.M.; Pang, S.F.; Qu, S.; Wang, Y.P. Identification of anti-inflammatory components in *Panax ginseng* of Sijunzi Decoction based on spectrum-effect relationship. *Chin. Herb. Med.* **2023**, *15*, 123–131. [CrossRef]
5. Liu, Z.; Li, Y.; Li, X.; Ruan, C.C.; Wang, L.J.; Sun, G.Z. The effects of dynamic changes of malonyl ginsenosides on evaluation and quality control of *Panax ginseng* C.A. Meyer. *J. Pharm. Biomed. Anal.* **2012**, *64–65*, 56–63. [CrossRef]
6. Lee, S.K.; Kim, J.H.; Sohn, H.J.; Yang, J.W. Changes in aroma characteristics during the preparation of red ginseng estimated by electronic nose, sensory evaluation and gas chromatography/mass spectrometry. *Sens. Actuators B Chem.* **2005**, *106*, 7–12. [CrossRef]
7. Li, L.; Yang, T.; Redden, R.; He, W.F.; Zong, X.X. Soil fertility map for food legumes production areas in China. *Sci. Rep.* **2016**, *6*, 26102. [CrossRef]

8.   Zhao, W.H.; Bi, X.J.; Peng, Y.Z.; Bai, M. Research advances of the phosphorus-accumulating organisms of *Candidatus* Accumulibacter, *Dechloromonas* and *Tetrasphaera*: Metabolic mechanisms, applications and influencing factors. *Chemosphere* **2022**, *301 Pt 1*, 135675. [CrossRef]

9.   Sehar, S.; Adil, M.F.; Ma, Z.X.; Karim, M.F.; Faizan, M.; Zaidi, S.S.A.; Siddiqui, M.H.; Alamri, S.; Zhou, F.R.; Shamsi, I.H. Phosphorus and *Serendipita indica* synergism augments arsenic stress tolerance in rice by regulating secondary metabolism related enzymatic activity and root metabolic patterns. *Ecotoxicol. Environ. Saf.* **2023**, *256*, 114866. [CrossRef]

10.   Zou, T.; Zhang, X.; Davidson, E.A. Global trends of cropland phosphorus use and sustainability challenges. *Nature* **2022**, *611*, 81–87. [CrossRef]

11.   Barra, P.J.; Duran, P.; Delgado, M.; Viscardi, S.; Claverol, S.; Larama, G.; Dumount, M.; Mora, M.D.L.L. Proteomic response to phosphorus deficiency and aluminum stress of three aluminum-tolerant phosphobacteria isolated from acidic soils. *iScience* **2023**, *26*, 207910. [CrossRef]

12.   Panigrahy, M.; Rao, D.N.; Sarla, N. Molecular mechanisms in response to phosphate starvation in rice. *Biotechnol. Adv.* **2009**, *27*, 389–397. [CrossRef]

13.   Xue, C.W.; Li, W.F.; Shen, R.F.; Lan, P. PERK13 modulates phosphate deficiency-induced root hair elongation in *Arabidopsis*. *Plant Science* **2021**, *312*, 111060. [CrossRef]

14.   Wu, Y.H.; Zhao, C.; Zhao, X.K.; Yang, L.Y.; Liu, C.; Jiang, L.Y.; Liu, G.D.; Liu, P.D.; Luo, L.J. Multi-omics-based identification of purple acid phosphatases and metabolites involved in phosphorus recycling in stylo root exudates. *Int. J. Biol. Macromol.* **2023**, *241*, 124569. [CrossRef]

15.   Li, D.W.; Tan, J.Z.; Li, Z.F.; Ou, L.J. Membrane lipid remodeling and autophagy to cope with phosphorus deficiency in the dinoflagellate *Prorocentrum shikokuense*. *Chemosphere* **2023**, *349*, 140844. [CrossRef]

16.   Zhang, H.C.; Wang, L.; Jin, X.L. High-throughput phenotyping of plant leaf morphological, physiological, and biochemical traits on multiple scales using optical sensing. *Crop J.* **2023**, *11*, 1303–1318. [CrossRef]

17.   Geng, Z.D.; Lu, Y.R.; Duan, L.F.; Chen, H.F.; Wang, Z.H.; Zhang, J.; Liu, Z.; Wang, X.M.; Zhai, R.F.; Ouyang, Y.D.; et al. High-throughput phenotyping and deep learning to analyze dynamic panicle growth and dissect the genetic architecture of yield formation. *Crop Environ.* **2024**, *3*, 1–11. [CrossRef]

18.   Mukul, M.M. Genetic analyses of morphological traits, and phenotypic screening of tossa jute germplasm grown under salinity stress. *Heliyou* **2023**, *9*, e12448. [CrossRef]

19.   Silva, P.C.; Sánchez, A.C.; Opazo, M.A.; Mardones, L.A.; Acevedo, E.A. Grain yield, anthesis-silking interval, and phenotypic plasticity in response to changing environments: Evaluation in temperate maize hybrids. *Field Crops Res.* **2022**, *285*, 108583. [CrossRef]

20.   Patel, M.; Rangani, J.; Kumari, A.; Parida, A.K. Mineral nutrient homeostasis, photosynthetic performance, and modulations of antioxidative defense components in two contrasting genotypes of *Arachis hypogaea* L. (peanut) for mitigation of nitrogen and/or phosphorus starvation. *J. Biotechnol.* **2020**, *323*, 136–158. [CrossRef]

21.   Zhang, S.F.; Dai, B.J.; Wang, Z.H.; Qaseem, M.F.; Li, H.L.; Wu, A.M. The key physiological and molecular responses of *Neolamarckia cadamba* to phosphorus deficiency stress by hydroponics. *Ind. Crops Prod.* **2023**, *202*, 117065. [CrossRef]

22.   Wang, S.; Zheng, S.W.; Bian, T.; Wu, T.; Li, X.X.; Fu, H.D.; Sun, Z.P.; Li, T.L. Photosynthetic characteristics combined with metabolomics analysis revealed potential mechanisms of cucumber (*Cucumis sativus*) yield reduction induced by different phosphorus stresses. *Sci. Hortic.* **2022**, *302*, 111156. [CrossRef]

23.   Hu, T.L.; Zhang, Y.H.; Wang, H.; Jin, H.Y.; Liu, B.J.; Lin, Z.B.; Ma, J.; Wang, X.J.; Liu, Q.; Liu, H.T.; et al. Biological nitrogen fixation in rice paddy soils is driven by multiple edaphic factors and available phosphorus is the greatest contributor. *Pedosphere*, 2023; *in press*. [CrossRef]

24.   Gu, R.L.; Chen, F.J.; Long, L.Z.; Cai, H.G.; Liu, Z.G.; Yang, J.B.; Wang, L.F.; Li, H.Y.; Li, J.H.; Liu, W.X.; et al. Enhancing phosphorus uptake efficiency through QTL-based selection for root system architecture in maize. *J. Genet. Genom.* **2016**, *43*, 663–672. [CrossRef]

25.   Mo, X.H.; Zhang, M.K.; Liang, C.Y.; Cai, L.Y.; Tian, J. Integration of metabolome and transcriptome analyses highlights soybean roots responding to phosphorus deficiency by modulating phosphorylated metabolite processes. *Plant Physiol. Biochem.* **2019**, *139*, 397–706. [CrossRef]

26.   Asif, I.; Dong, Q.; Wang, X.R.; Li, X.L.; Li, M.J.; Yang, Y.Z.; Zhou, J.; Wei, Q.P.; Zhou, B.B. Integrative physiological, transcriptome and metabolome analysis reveals the involvement of carbon and flavonoid biosynthesis in low phosphorus tolerance in cotton. *Plant Physiol. Biochem.* **2023**, *196*, 302–317.

27.   He, F.L.; Hu, S.Y.; Liu, R.T.; Li, X.X.; Guo, S.Q.; Wang, H.; Tian, G.; Qi, Y.T.; Wang, T.T. Decoding the biological toxicity of phenanthrene on intestinal cells of *Eisenia fetida*: Effects, toxicity pathways and corresponding mechanisms. *Sci. Total Environ.* **2023**, *904*, 166903. [CrossRef]

28.   Zhang, Z.Z.; Zhang, Z.D.; Han, X.Y.; Wu, J.H.; Zhang, L.Z.; Wang, J.R.; Wang-Pruski, G.F. Specific response mechanism to autotoxicity in melon (*Cucumis melo* L.) root revealed by physiological analyses combined with transcriptome profiling. *Ecotoxicol. Environ. Saf.* **2020**, *200*, 110779. [CrossRef]

29.   Lv, L.; Zhang, Y.Y.; Sun, H.; Zuo, X.X.; Wu, C.; Qian, J.Q. Effects of phosphorus stress on nutrients and saponins in ginseng plants. *J. Jilin Agric. Univ.* **2023**, *45*, 307–315.

30. Shen, C.; Huang, B.F.; Hu, L.; Yuan, H.W.; Huang, Y.Y.; Wang, Y.B.; Sun, Y.F.; Li, Y.; Zhang, J.R.; Xin, J.L. Comparative transcriptome analysis and Arabidopsis thaliana overexpression reveal key genes associated with cadmium transport and distribution in root of two *Capsicum annuum* cultivars. *J. Hazard. Mater.* **2024**, *465*, 133365. [CrossRef]

31. The Pharmacopoeia Commission of the People's Republic of China. *Pharmacopoeia of the People's Republic of China*, 2020th ed.; Chinese Medical Science and Technology Publishers: Beijing, China, 2015.

32. Lei, H.X.; Zhang, H.F.; Zhang, Z.H.; Sun, H.; Li, M.J.; Shao, C.; Liang, H.; Wu, H.P.; Zhang, Y.Y. Physiological and transcriptomic analyses of roots from *Panax ginseng* C. A. Meyer under drought stress. *Ind. Crops Prod.* **2023**, *191*, 115858. [CrossRef]

33. Wei, G.F.; Yang, F.; Wei, F.G.; Zhang, L.J.; Gao, Y.; Qian, J.; Chen, Z.J.; Jia, Z.W.; Wang, Y.; Su, H.; et al. Metabolomes and transcriptomes revealed the saponin distribution in root tissues of *Panax quinquefolius* and *Panax notoginseng*. *J. Ginseng Res.* **2020**, *44*, 757–769. [CrossRef]

34. Herrera-Estrella, L.; López-Arredondo, D. Phosphorus: The underrated element for feeding the world. *Trends Plant Sci.* **2016**, *21*, 461–463. [CrossRef]

35. Dey, P.; Santhi, R.; Maragatham, S.; Sellamuthu, K. Status of phosphorus and potassium in the Indian soils vis-à-vis world soils. *Indian J. Fertil.* **2017**, *13*, 44–59.

36. Tung, A.; Levin, M. Extra-genomic instructive influences in morphogenesis: A review of external signals that regulate growth and form. *Dev. Biol.* **2020**, *461*, 1–12. [CrossRef]

37. Wu, C.; Li, B.C.; Wei, Q.; Pan, Q.; Zhang, W.Y. Endophytic fungus *Serendipita indica* increased nutrition absorption and biomass accumulation in *Cunninghamia lanceolata* seedlings under low phosphate. *Acta Ecol. Sin.* **2019**, *39*, 21–29. [CrossRef]

38. Akash Parida, A.P.; Srivastava, A.; Mathur, S.; Sharma, A.K.; Kumar, R. Identification, evolutionary profiling, and expression analysis of F-box superfamily genes under phosphate deficiency in tomato. *Plant Physiol. Biochem.* **2021**, *162*, 349–362. [CrossRef]

39. Li, L.Y.; Yang, H.M.; Liu, P.; Ren, W.B.; Wu, X.H.; Huang, F. Combined impact of heat stress and phosphate deficiency on growth and photochemical activity of sheepgrass (*Leymus chinensis*). *J. Plant Physiol.* **2018**, *231*, 271–276. [CrossRef]

40. Yang, Y.X.; Yao, P.P.; Song, H.; Li, Q.C. NtNCED3 regulates responses to phosphate deficiency and drought stress in *Nicotiana tabacum*. *Gene* **2023**, *872*, 147458. [CrossRef]

41. Zheng, Q.M.; Hu, J.L.; Dong, C.F.; Hu, H.; Zhao, C.F.; Lei, K.Q.; Tian, Z.W.; Dai, T.B. Differences in membrane lipid homeostasis confer contrast tolerance to low phosphorus in two wheat (*Triticum aestivum* L.) cultivars. *Environ. Exp. Bot.* **2024**, *219*, 105653. [CrossRef]

42. Maxwell, K.; Johnson, G.N. Chlorophyll fluorescence—A practical guide. *J. Exp. Bot.* **2000**, *51*, 659–668. [CrossRef]

43. Sayed, O.H. Chlorophyll Fluorescence as a Tool in Cereal Crop Research. *Photosynthetica* **2003**, *41*, 321–330. [CrossRef]

44. Zhang, Y.; Liu, G.J. Effects of cesium accumulation on chlorophyll content fluorescence of *Brassica juncea*, L.J. *Environ. Radioact.* **2018**, *195*, 26–32. [CrossRef] [PubMed]

45. Shen, Y.F.; Tu, Z.H.; Zhang, Y.L.; Zhong, W.P.; Xia, H.; Hao, Z.Y.; Zhang, C.G.; Li, H.G. Predicting the impact of climate change on the distribution of two relict *Liriodendron* species by coupling the MaxEnt model and actual physiological indicators in relation to stress tolerance. *J. Environ. Manag.* **2022**, *332*, 116024. [CrossRef] [PubMed]

46. Huang, Z.; Liu, Y.; Tian, F.P.; Wu, G.L. Soil water availability threshold indicator was determined by using plant physiological responses under drought conditions. *Ecol. Indic.* **2020**, *118*, 106740. [CrossRef]

47. Ben, Y.; Cheng, M.Z.; Liu, Y.Q.; Wang, X.; Wang, L.H.; Yang, Q.; Huang, X.H.; Zhou, Q. Biomarker changes and oxidative damage in living plant cells as new biomonitoring indicators for combined heavy metal stress assessment. *Ecol. Indic.* **2023**, *154*, 110784. [CrossRef]

48. Javidi, M.; Maali-Amiri, R.; Poormazaheri, H.; Niaraki, M.S.; Kariman, K. Cold stress-induced changes in metabolism of carbonyl compounds and membrane fatty acid composition in chickpea. *Plant Physiol. Biochem.* **2022**, *192*, 10–19. [CrossRef] [PubMed]

49. Wei, L.X.; Xu, D.D.; Zhou, L.J.; Chen, H.; Peng, Z.W.; Chen, G.Y.; Wang, L.H.; Cao, H.S.; Peng, Y.Q.; Geng, S.Y.; et al. The critical role of CmCIPK1-CmRbohD1/D2 complexes in generating H_2O_2 signals for enhancing salt tolerance in pumpkins. *Hortic. Plant J.* 2024; *in press*. [CrossRef]

50. Han, Y.C.; Liu, N.; Li, C.; Wang, S.W.; Jai, L.H.; Zhang, R.; Li, H.; Tan, J.F.; Xue, H.W.; Zheng, W.M. TaMADS2-3D, a MADS transcription factor gene, regulates phosphate starvation responses in plants. *Crop J.* **2022**, *10*, 243–253. [CrossRef]

51. Mai NT, P.; Mai, C.D.; Ngyyen, H.V.; Le, K.Q.; Duong, L.V.; Tran, T.A.; To, H.T.M. Discovery of new genetic determinants of morphological plasticity in rice roots shoots under phosphate starvation using, G.W.A.S. *J. Plant Physiol.* **2021**, *257*, 153340. [PubMed]

52. Devaiah, B.N.; Madhuvanthi, R.; Karthikeyan, A.S.; Raghothama, K.G. Phosphate starvation responses and gibberellic acid biosynthesis are regulated by the MYB62 Transcription Factor in *Arabidopsis*. *Mol. Plant* **2009**, *2*, 43–58. [CrossRef]

53. Nazari, M.; Ghasemi-Soloklui, A.A.; Kordrostami, M.; Latef, A.A.H.A. Deciphering the response of medicinal plants to abiotic stressors: A focus on drought and salinity. *Plant Stress* **2023**, *10*, 100255. [CrossRef]

54. Wu, J.J.; Liu, X.Y.; Ge, F.; Li, N. Tolerance mechanism of rice (*Oryza sativa* L.) seedings towards polycyclic aromatic hydrocarbons toxicity: The activation of SPX-mediated signal transduction to maintain *P. homeostasis*. *Environ. Pollut.* **2024**, *341*, 123009. [CrossRef] [PubMed]

55. Hatem, R.; Bulak, A.A.; Yves, P. Regulation of phosphate starvation responses in plants: Signaling players and cross-talks. *Mol. Plant* **2010**, *3*, 288–299.

56. Wang, L.; Deng, M.J.; Xu, J.M.; Zhu, X.L.; Mao, C.Z. Molecular mechanisms of phosphate transport and signaling in higher plants. *Semin. Cell Dev. Biol.* **2018**, *74*, 114–122. [CrossRef] [PubMed]

57. Baek, D.; Chun, H.J.; Yun, D.J.; Kim, M.C. Cross-talk between phosphate starvation and other environmental stress signaling pathways in plants. *Mol. Cells* **2017**, *40*, 697–705. [CrossRef] [PubMed]

58. Shukla, D.; Waigel, S.; Rouchka, E.C.; Sandhu, G.; Trivedi, P.K.; Sahi, S.V. Genome-wide expression analysis reveals contrasting regulation of phosphate starvation response (PSR) in root and shoot of *Arabidopsis* and its association with biotic stress. *Environ. Exp. Bot.* **2021**, *188*, 104483. [CrossRef]

59. Yan, H.M.; Wang, Y.L.; Chen, B.; Lv, C.W.; Li, J.Z.; Zhao, Q.Z. OsCKX2 regulates phosphate deficiency tolerance by modulating cytokinin in rice. *Plant Sci.* **2022**, *319*, 111257. [CrossRef] [PubMed]

60. Prathap, V.; Kumar, S.; Meena, N.; Maheshwari, C.; Dalal, M.; Tyagi, A. Phosphorus Starvation Tolerance in Rice Through Combined Physiological, Biochemical, and Proteome Analyses. *Rice Sci.* **2023**, *30*, 613–631. [CrossRef]

61. Zhu, Z.X.; Qu, K.Z.; Li, D.; Zhang, L.X.; Wang, C.Y.; Cong, L.; Bai, C.M.; Lu, X.C. SbPHO2, a conserved Pi starvation signalling gene, is involved in the regulation of the uptake of multiple nutrients in sorghum. *Plant Sci.* **2023**, *327*, 111556. [CrossRef] [PubMed]

62. Ramaiah, M.; Jain, A.; Yugandhar, P.; Raghothama, K.G. ATL8, a RING E3 ligase, modulates root growth and phosphate homeostasis in Arabidopsis. *Plant Physiol. Biochem.* **2022**, *179*, 90–99. [CrossRef]

63. Wang, B.; Gao, Z.Y.; Shi, Q.H.; Gong, B. SAMS1 stimulates tomato root growth and P availability via activating polyamines and ethylene synergetic signaling under low-P condition. *Environ. Exp. Bot.* **2022**, *197*, 104844. [CrossRef]

64. Zhang, Y.X.; Wang, Y.Q.; Guo, Y.Y.; Chen, Y.; Sun, Y.P.; Wang, Z.L.; Guan, L.X.; Wang, L.; Chen, L.L. Multi-omics profiling reveals the effects of hydrogen peroxide treatment on carbohydrate and energy metabolism in postharvest broccoli. *Postharvest Biol. Technol.* **2024**, *209*, 112703. [CrossRef]

65. Xie, L.Y.; Xu, Y.B.; Ding, X.Q.; Liang, S.; Li, D.L.; Fu, A.K.; Zhan, X.A. Itaconic acid and dimethyl itaconate exert antibacterial activity in carbon-enriched environments through the TCA cycle. *Biomed. Pharmacother.* **2023**, *167*, 115487. [CrossRef] [PubMed]

66. Yang, Z.H.; Xue, B.H.; Song, G.L.; Shi, S.Q. Effects of citric acid on antioxidant system and carbon-nitrogen metabolism of *Elymus dahuricus* under Cd stress. *Ecotoxicol. Environ. Saf.* **2022**, *233*, 113321. [CrossRef] [PubMed]

67. Shan, S.Z.; Wang, S.S.; Yan, X.; Chen, K.; Liang, L.; Li, X.H.; Zhou, C.X.; Yan, X.J.; Ruan, R.; Cheng, P.F. Mixotrophic culture of *Chaetoceros sp.* and the synergistic carbon and energy metabolism. *Bioresour. Technol.* **2023**, *390*, 129912. [CrossRef] [PubMed]

68. Liu, J.; Yang, J.; Zhang, S.Y.; Gao, J.Q.; Li, X.; Zhou, J.H.; Hu, L.; Huang, L.Q. Metabolome and transcriptome analyses identify the underground rhizome growth through the regulation of rhizome apices in *Panax ginseng*. *Ind. Crops Prod.* **2023**, *206*, 1176354. [CrossRef]

69. Kochan, E.; Sienkiewicz, M.; Szmajda-Krygier, D.; Balcerczak, E.; Szymańska, G. Thymol as a control factor of the expression of key genes of the ginsenoside biosynthesis pathway and its effect on the production of ginseng saponins in Panax quinquefolium hairy root cultures. *Ind. Crops Prod.* **2024**, *210*, 118151. [CrossRef]

70. Koo, H.; Lee, Y.S.; Nguyen, V.B.; Giang, V.N.G.; Koo, H.J.; Park, H.S.; Mohanan, P.; Song, Y.H.; Ryu, B.; Kang, K.B.; et al. Comparative transcriptome and metabolome analyses of four *Panax* species explore the dynamics of metabolite biosynthesis. *J. Ginseng Res.* **2023**, *47*, 44–53. [CrossRef]

71. Schmiderer, C.; Grausgruber-Gröger, S.; Grassi, P.; Steinborn, R.; Novak, J. Influence of gibberellin and daminozide on the expression of terpene synthases and on monoterpenes in common sage (*Salvia officinalis*). *J. Plant Physiol.* **2010**, *167*, 779–786. [CrossRef]